Volume 1 | Number 1 | Jan 2013 | Pages 1–100

Nanoscale

www.rsc.org/nanoscale

ROYAL SOCIETY OF CHEMISTRY

ROYAL SOCIETY OF CHEMISTRY

www.rsc.org/nanoscale

Journal Name

Dynamic Article Links ▶

ARTICLE TYPE

Metal-organic framework as a chemical guide to control hydrogen desorption pathways of ammonia borane

Hyung Mo Jeong, ‡[a] Weon Ho Shin, ‡[a] Jung Hyo Park,[a] Jung Hoon Choi,[a] and Jeung Ku Kang[a,b,*]

We report that ammonia borane with a high uptake capacity for hydrogen can be encapsulated in a metal-organic framework (MOF) via capillary action, where the MOF functions as a chemical guide to control the hydrogen
10 **desorption pathways of ammonia borane by releasing only pure hydrogen, lowering its hydrogen desorption temperature, and suppressing its volumetric expansion during hydrogen desorption.**

The development of high uptake capacity hydrogen storage
15 materials is of great attention in that it could allow realization of hydrogen-fuel devices. As of now, hydrogen storage methods such as a high-pressure hydrogen tank, liquid hydrogen storage, absorption of molecular hydrogen on high surface areas materials, metal hydrides, and chemical hydrides have previously been
20 studied.[1,2] Meanwhile, the methods including high pressurized tanks, liquid hydrogen, and sorption materials still suffer from the very expensive costs attributed to extremely low temperature conditions. The other cases such as chemical hydride storages are in that they require a very high temperature to release a large
25 amount of hydrogen enabling practical applications.

In principle, ammonia borane (AB), NH_3BH_3, is a very promising potential candidate as a hydrogen storage material in that it has the high uptake capacity of 19.6 wt.% and its excellent stability in air.[1-5] However, there are several challenging issues
30 related to use AB for advanced applications, which includes 1) further reducing the hydrogen-releasing temperature less than 110 ^oC that AB can release hydrogen at the usual condition, 2) to suppressing detrimental by-products such as borazine ($B_3N_3H_6$), and 3) preventing the volumetric expansion of the hydrogen-
35 adsorbing product. To solve the above issues, many different approaches have been studied, including the use of the ball-milling under the presence of transition of Co, Ni or alkaline metals.[6-13] Despite these efforts, the solutions are still far from satisfying the above requirements.
40 A metal-organic framework (MOF) has been of a great attention because its having the capability to capture the selective molecules.[14,15] In addition, the enhanced dehydrogenation properties by confinement of the AB in various MOFs have been also reported.[13,16-22] In particular, the MOF-5,[14,15,23,24] composed
45 of Zn_4O nodes and 1,4-benzenedicarboxylate, is one of the most important materials in that it has been on the fundamental conceptual structure for synthesis of other many different MOF structures. Herein, we report the ammonia borane-encapsulated

MOF-5 (AB@MOF-5) structure and find that the AB molecules
50 confined in the MOF-5 structure provide improved performance for hydrogen desorption. Moreover, we find that the MOF-5 itself acts as a chemical guide, similar to the catalyst, to selectively control the chemical pathway among many competing reactions. Scheme 1 shows the proposed idea about how to selectively
55 control the reaction using AB encapsulated inside the confined nanometer scale sized cage of the MOF-5.
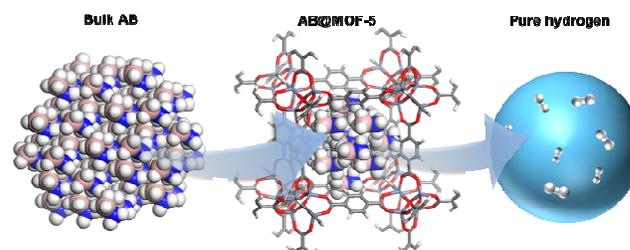
Scheme 1 The schematic structure of the confined AB-encapsulated inside the MOF-5(AB@MOF-5). The AB@MOF-5 releases pure
60 hydrogen.

The AB@MOF-5 was prepared by the chemical impregnation method, where the AB-resolved methanol solution was evaporated at room temperature in the presence of MOF-5 crystals. Our analyses indicate clearly that the inter-space of the
65 MOF-5 is filled with AB. First of all, the transparent yellowish colored MOF-5 crystal changed into the opaque white colored crystal. This provides the direct evidence that AB is encapsulated inside the MOF-5. Secondly, the scanning electron microscopy (SEM) images, as seen in Fig. S1, demonstrate that there is no
70 structural change after confining AB in the MOF-5 structure. Meanwhile, the detailed observation of the AB@MOF-5 image shows small particles on the surface of the MOF-5. Furthermore, the Brunauer Emmett Teller (BET) specific surface areas of MOF-5 and AB@MOF-5 are proven to be 2169 m^2/g and 7 m^2/g,
75 respectively, as seen from the isotherms in Fig. 1. The decrement of the specific surface area after formation of AB in the MOF-5 structure is attributed to AB encapsulated into the micropores of the MOF-5. This result is also consistent with the XRD patterns of pristine MOF-5, AB@MOF-5 before dehydrogenation, and
80 AB@MOF-5 after dehydrogenation, as shown in Fig. S2. In addition, pore size distribution of MOF-5, in Fig 1c shows that the pore size is about 1.3 nm and the total pore volume is 0.1 cc/g that can accommodate a large amount of AB. Meanwhile, the

Nanoscale Accepted Manuscript

pore size distribution of AB@MOF-5 in Fig. 1d supports that the micropores of MOF-5 were filled with AB and the total pore volume is sharply decreased to 0.14 cc/g. This supports that the MOF-5 with a large surface area can encapsulate the largest amount loading of AB, compared to those on previous reports for AB composites with the Mg-MOF-74 having ~1.2 nm hexagonal channels,[13] the Y-based MOF having ~0.6 nm channels,[18] and Ni-based MOFs having amorphous Ni sites.[19]

Furthermore, the decreased intensity of the main peak due to the encapsulation of the AB is recovered partially after the hydrogen desorption. It is indicated that the MOF-5 in samples is expected to act as a proper scaffold to control hydrogen desorption pathways of AB.
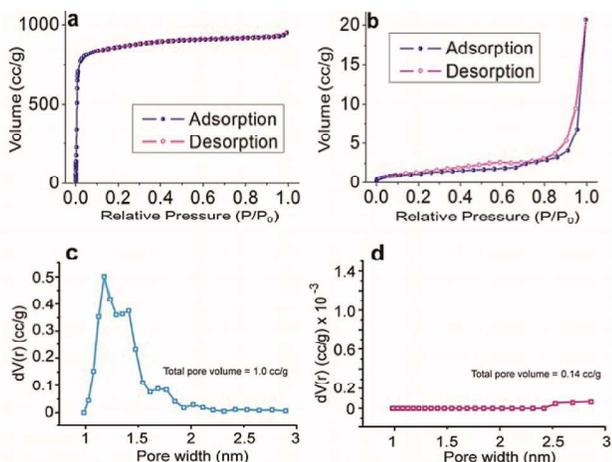

Fig. 1 N$_2$ adsorption (blue) and desorption (pink) isotherms at 77 K of a. the MOF-5 and b. the AB@MOF-5. Pore size distribution of c. the MOF-5 and d. the AB@MOF-5.

Also, to investigate thermal decomposition properties of pure AB and AB@MOF-5, the thermogravimetric analysis (TGA) and the mass spectroscopy (MS) measurement have been performed. A pure AB is proven to release hydrogen from 110 ^{o}C. However, when AB is confined in a nanometer scale sized cage of the MOF-5, the mass drop is found to start from around 55 ^{o}C while the major mass drop occurs at around 100 ^{o}C.

The total mass drop of the AB@MOF-5 was about 5.3 wt.% (See Fig. 2a). It is easily expected that the initial mass drop of AB@MOF-5 at around 55 to 100°C originate from evaporations of the residual water and solvent. Meanwhile, to reveal the cause of major mass loss of AB@MOF-5 at the temperature between 100-200°C, the released gases have been analysed by the MS apparatus. Interestingly, we found out that the AB@MOF-5 releases only hydrogen, while borazine or any other element has not been detected. This is quite different from those of a pure AB where high levels of borazine and hydrogen were contained in the released gas of a pure AB (Fig. 2b,c).[6-12] Moreover, other gases except hydrogen, which are also plausible to be generated during hydrogen desorption, were not detected from the TGA-MS analysis (Fig. S3). Consequently, excepting the mass drop at 50 to 100 ^{o}C from evaporations of residual solvent and water, these results support that the 4.4 wt. % of mass drop of the AB@MOF-5 in TGA corresponds to the total mass of only released hydrogen during thermal decomposition of AB in the MOF-5.

The TGA-MS data in Fig. 2 suggest that the AB@MOF-5 has the enhanced kinetics for hydrogen desorption. Also, to unveil the

nature for hydrogen generation kinetics, the desorption activation energy was determined by the following equation of

$$\ln(T_p^2/\beta) = E_a/RT_p + \ln(E_a A_0/RC)$$

in which T_p is the temperature of peak position, β is the heating rate, E_a is the activation energy, R is the gas constant, A_0 is the quantity adsorbed, and C is the constant relating to the desorption rate. Fig. 3a shows the temperature programmed desorption (TPD) spectra of AB@MOF-5 at various heating rates and the Amenomiya plot is also determined as seen in Fig. 3b. The desorption activation energy (Ea) of the AB@MOF-5 is calculated to be 64.3 kJ/mol, which is much lower than the 184 kJ/mol from a bulk AB and the 131 kJ/mol to 160 kJ/mol from Ni-based MOFs.[19] This value of 64.3 kJ/mol provides the clear evidence for the enhanced kinetics of hydrogen desorption with the AB@MOF-5 compared to pristine bulk AB and AB/MOFcats structures. In addition, it is considered that the catalytic behaviour[19,20] by Zn ions in MOF-5 could be one of other reasonable keys to the enhanced decomposition reactions of AB@MOF-5.
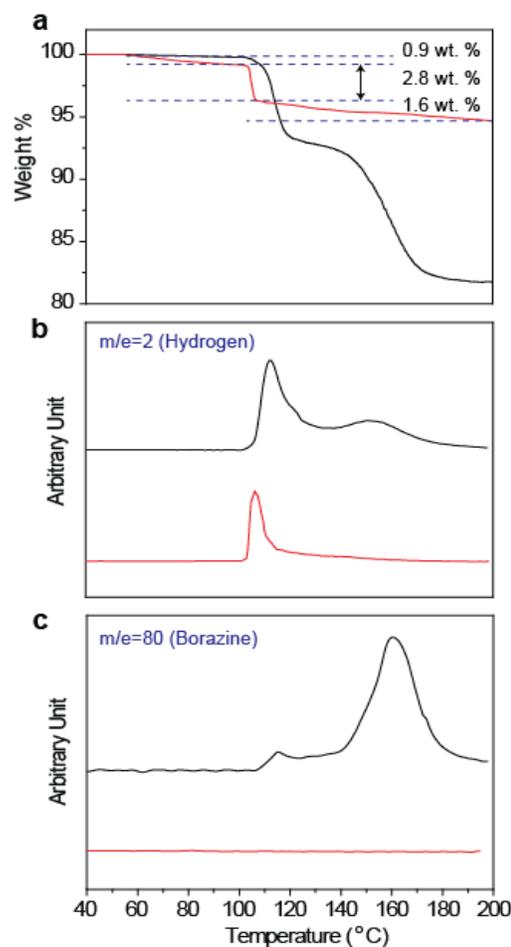

Fig. 2 Thermal decomposition properties of bulk AB (black lines) and AB@MOF-5 (red lines) samples: a. TGA spectra, b. MS for m/e=2 (hydrogen), c. MS for m/e=80 (borazine)

The amount of borazine results in a significant mass drop of a bulk AB. However, using the MOF-5 as a scaffold to confine AB

gives an important clue to control desorption reaction pathways of AB. It is considered that the confined AB could reduce the desorption temperature for hydrogen energetically unstabilized by its confinement. In addition, the selective hydrogen release is also attributed to the role of the MOF-5 as the chemical reaction guide to selectively suppress the certain chemical reaction pathway. The detailed mechanism has been discussed in the next paragraph. It should be noted that all our procedures related to synthesis of the AB@MOF-5 are performed at ambient conditions and the properties of the AB@MOF-5 remain for several weeks, where the AB@MOF-5 is tightly sealed in a glass vial. The AB powder after resolving and evaporating methanol without any additional media was tested for the controlled study, but its thermal decomposition properties have been maintained as those of a pure AB. Therefore, we can conclude that the enhanced hydrogen desorption properties come from the confined structure of the MOF-5.
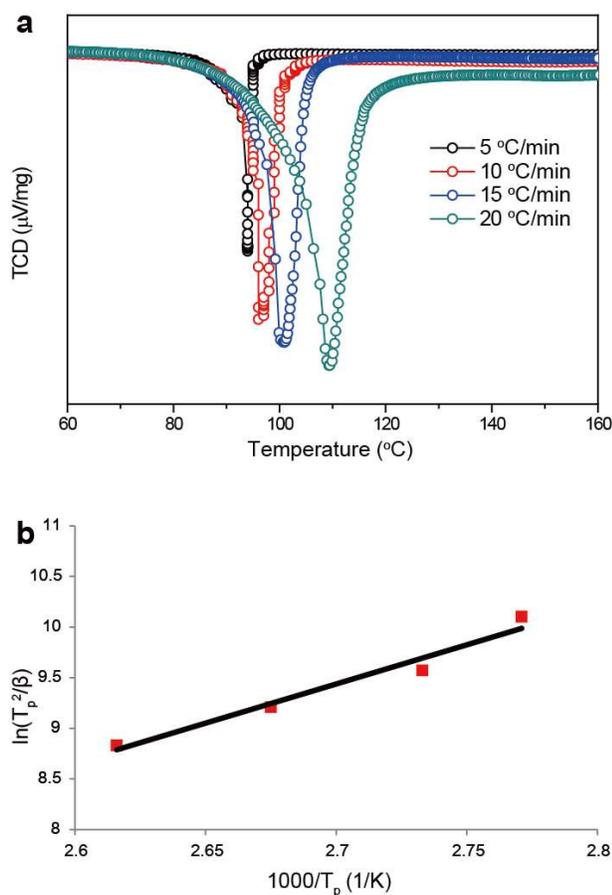

Fig. 3 a. The Temperature programed desorption (TPD) spectrum of the AB@MOF-5. b. The hydrogen desorption kinetics from Amenomiya equation.

Fig. 4 shows the photographs of pure AB and AB@MOF-5 samples before and after heating to 200 °C which allows a complete release of hydrogen. The pure AB was found to be expanded severely and swelled in the alumina boat, while the AB@MOF-5 maintains its volume after thermal decomposition.

The pure AB decomposes through two step-wise reactions.[25-27] The first reaction starts at 110 °C, which produces polyaminoborane (PAB, $[NH_2BH_2]_n$) and hydrogen. Next, in the second reaction, the PAB decomposes at a temperature of about 120 °C that produces hydrogen in addition to two different products of polyiminoborane (PIB, $[NHBH]_n$) and borazine. If one could design to allow only the selective generation of pure hydrogen, it is necessary to control the chemical reaction by suppressing the borazine-generating reaction, but by facilitating the PIB formation. As we have already discussed, the AB@MOF-5 is found to selectively suppress the generation of borazine as the product. Also, to explore the detailed mechanism for the thermal decomposition of the AB@MOF-5, we performed [11]B magic angle spinning (MAS) solid state nuclear magnetic resonance (NMR) spectroscopy measurements. First of all, the ^{11}B NMR spectra for bulk AB and AB@MOF-5 samples revealed a boron species with the chemical shift of -26.7 ppm (Fig. 4c), corresponding to the chemical shift for the structure of AB. Again, this confirms that the AB exists inside the MOF-5 without any chemical change. After hydrogen release, the peak of -26.7 ppm diminished and 1.4 ppm, 11.6 ppm, and 22.3 ppm peaks were newly created. However, the hydrogen-released AB@MOF-5 shows only 1.4 ppm and 12.2 ppm peaks (Fig. 4d). The 22.3 ppm peak,[11] which could be assigned to polyborazylene, did not appear. The other peaks shifted slightly onto the left side, which arose due to the confinement in the MOF-5 structure. According to these results, the mechanism for releasing hydrogen from the AB@MOF-5 without the release of any other gas implies that the chemical reaction for producing borazine did not occur, while just the reaction for producing PIB occurs selectively.
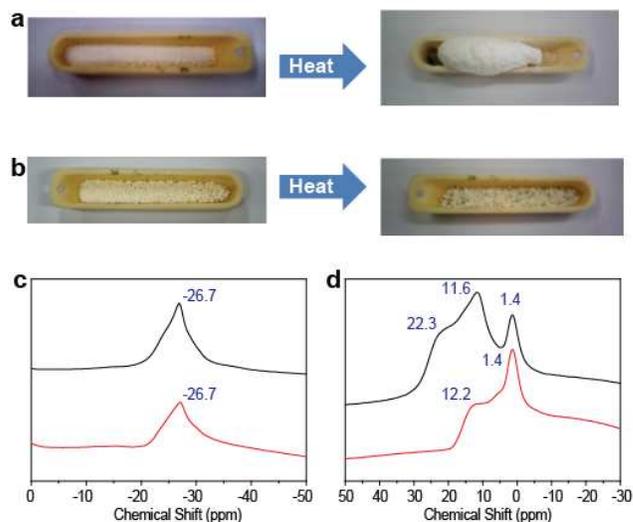

Fig. 4 Photographs of samples before and after heating to 200 °C: a. Pure AB at a bulk state, b. The AB@MOF-5. Solid state ^{11}B NMR spectra of pure AB (black lines) and AB@MOF-5 (red lines) samples c. before hydrogen release, d. after hydrogen release. The exact chemical shifts are displayed on the figures.

Therefore, we conclude that the MOF-5 acts as a chemical guide to selectivly control the hydrogen desorption reaction pathway. The PIB is a linearly linked polymer structure, while borazine is a ring structure like benzene. In terms of the space required for formation of PIB and borazine, PIB is energetically preferred in the nanopores of the MOF-5. Moreover, the

theoretical study[26] supports that borazine is on a thermodynamically less stable structure than PIB. The small size of the pores and channels in the MOF-5 could make it harder to form borazine during thermal decomposition. Thus, the AB@MOF-5 could release only hydrogen without any other detrimental by-product. This finding could gives us a new clue to manipulate the chemical reaction pathway for hydrogen desorption oof a high-capacity chemical hydride.

Conclusions

In summary, we have synthesized a new AB@MOF-5. It was proven that the MOF-5 acts as a chemical guide to selectively control the hydrogen desorption reaction pathway of AB molecules. The hydrogen desorption mechanism from the AB@MOF-5 implies that the chemical reaction for producing borazine did not occur while just the reaction for producing PIB occurs selectively. In addition, the AB@MOF-5 is found to reduce its hydrogen desorption temperature and the volume change during thermal decomposition of the encapsulated AB is negligible, thus implying that the MOF-5 is suitable for the confinement of AB for enhanced hydrogen desorption kinetics. Consequently, these results demonstrate that a hydrogen desorption pathway of a AB molecule could be modified to selectively release only pure hydrogen with improved kinetics if it could be encapsulated inside suitable nanometer scale sized cages of MOFs.

Acknowledgement

Notes and references

a Department of Materials Science & Engineering and NanoCentury KAIST Institute, Korea Advanced Institute of Science and Technology, Daejeon 305-701, Republic of Korea. Fax: +82-42-350-3310; Tel: +82-42-350-3338; E-mail: jeungku@kaist.ac.kr
b Graduate School of Energy, Environment, Water, and Sustainability (EEWS), Korea Advanced Institute of Science and Technology, Daejeon 305-701, Republic of Korea.
Fax: +82-42-350-3310; Tel: +82-42-350-3338; E-mail: jeungku@kaist.ac.kr
‡ Hyung Mo Jeong and Weon Ho Shin contributed equally to this work.
† Electronic Supplementary Information (ESI) available: [details of any supplementary information available should be included here]. See DOI: 10.1039/b000000x/

1. T. B. Marder, *Angew. Chem. Int. Ed.*, 2007, **46**, 8116.
2. F. H. Stephens, V. Pons and R. T. Baker, *Dalton Trans.*, 2007, 2613.
3. B. Peng and J. Chen, *Energy Environ. Sci.*, 2008, **1**, 479.
4. C. W. Hamilton, R. T. Baker, A. Staubitz and I. Manners, *Chem. Soc. Rev.*, 2009, **38**, 279.
5. N. C. Smythe and J. C. Gordon, *Eur. J. Inorg. Chem.*, 2010, 509.
6. A. Gutowska, L. Y. Li, Y. S. Shin, C. M. M. Wang, X. H. S. Li, J. C. Linehan, R. S. Smith, B. D. Kay, B. Schmid, W. Shaw, M. Gutowski and T. Autrey, *Angew. Chem. Int. Ed.*, 2005, **44**, 3578.
7. M. E. Bluhm, M. G. Bradley, R. Butterick, U. Kusari and L. G. Sneddon, *J. Am. Chem. Soc.*, 2006, **128**, 7748.
8. F. Y. Cheng, H. Ma, Y. M. Li and J. Chen, *Inorg. Chem.*, 2007, **46**, 788.
9. X. D. Kang, Z. Z. Fang, L. Y. Kong, H. M. Cheng, X. D. Yao, G. Q. Lu and P. Wang, *Adv. Mater.*, 2008, **20**, 2756.
10. J. Spielmann, G. Jansen, H. Bandmann and S. Harder, *Angew. Chem. Int. Ed.*, 2008, **47**, 6290.
11. Z. T. Xiong, C. K. Yong, G. T. Wu, P. Chen, W. Shaw, A. Karkamkar, T. Autrey, M. O. Jones, S. R. Johnson, P. P. Edwards and W. I. F. David, *Nat. Mater.*, 2008, **7**, 138.
12. J. Z. Zhao, J. F. Shi, X. W. Zhang, F. Y. Cheng, J. Liang, Z. L. Tao and J. Chen, *Adv. Mater.*, 2009, **22**, 394.
13. S. Gadipelli, J. Ford, W. Zhou, H. Wu, T. J. Udovic and T. Yildirim, *Chem. Eur. J.*, 2011, **17**, 6043.
14. H. Li, M. Eddaoudi, M. O'Keeffe and O. M. Yaghi, *Nature*, 1999, **402**, 276.
15. S. Ma and H.-C. Zhou, *Chem. Commun.*, 2010, **46**, 44.
16. Z. Li, G. Zhu, G. Lu, S. Qiu and X. Yao, *J. Am. Chem. Soc.*, 2010, **132**, 1490.
17. Y. Li, P. Song, J. Zheng and X. Li, *Chem. Eur. J.*, 2010, **16**, 10887.
18. X.-l. Si, L.-x. Sun, F. Xu, C.-l. Jiao, F. Li, S.-s. Liu, J. Zhang, L.-f. Song, C.-h. Jiang, S. Wang, Y.-L. Liu and Y. Sawada, *International Journal of Hydrogen Energy*, 2011, **36**, 6698.
19. R.-Q. Zhong, R.-Q. Zou, T. Nakagawa, M. Janicke, T. A. Semelsberger, A. K. Burrell and R. E. Del Sesto, *Inorganic Chemistry*, 2012, **51**, 2728.
20. G. Srinivas, J. Ford, W. Zhou and T. Yildirim, *International Journal of Hydrogen Energy*, 2012, **37**, 3633.
21. G. Srinivas, W. Travis, J. Ford, H. Wu, Z.-X. Guo and T. Yildirim, *Journal of Materials Chemistry A*, 2013, **1**, 4167.
22. L. Gao, C.-Y. V. Li, H. Yung and K.-Y. Chan, *Chemical Communications*, 2013, **49**, 10629.
23. S. Hermes, M. K. Schroter, R. Schmid, L. Khodeir, M. Muhler, A. Tissler, R. W. Fischer and R. A. Fischer, *Angew. Chem. Int. Ed.*, 2005, **44**, 6237.
24. M. Muller, S. Hermes, K. Kahler, M. W. E. van den Berg, M. Muhler and R. A. Fischer, *Chem. Mater.*, 2008, **20**, 4576.
25. M. G. Hu, R. A. Geanangel and W. W. Wendlandt, *Thermochim. Acta*, 1978, **23**, 249.
26. C. R. Miranda and G. Ceder, *J. Chem. Phys.*, 2007, **126**.
27. A. C. Stowe, W. J. Shaw, J. C. Linehan, B. Schmid and T. Autrey, *Phys. Chem. Chem. Phys.*, 2007, **9**, 1831.

Table of contents
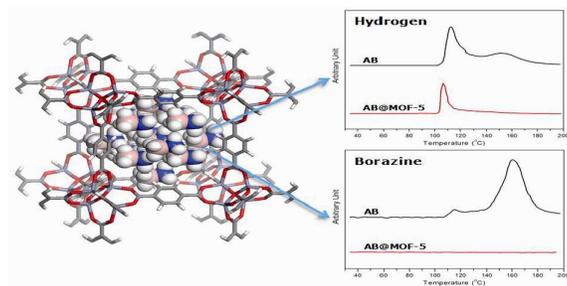
 The ammonia borane-encapsulated metal-organic framework-5 enables to provide the improved characteristics, where the MOF-5 acts as a chemical guide to control the hydrogen desorption reaction pathway.